



An Adaptively-damped Compressible-liquid Model for Non-cavitating Hydraulic Surges

R. J. Chandran*, R. Raju, A. Salih

Department of Aerospace Engineering, Indian Institute of Space Science and Technology, Thiruvananthapuram, Kerala, India

PAPER INFO

Paper history:

Received 09 May 2020

Received in revised form 22 June 2020

Accepted 03 August 2020

Keywords:

Two-equation Model
Hydraulic Surge
Compressible Liquid
Variable Friction Coefficient
Non-cavitating Flow
Adaptive Damping

ABSTRACT

This research presents a compact and computationally-efficient two-equation compressible-liquid model. The model is specifically developed for the numerical computation of hydraulic surges in pipes under high fluid pressure where cavitation is absent. The proposed model aims to simplify the three-equation model of Neuhaus et al. for two-phase cavitation hammers. Compressible effects in liquid during the transients are considered by including a suitable equation of state into the model. A tunable function of the relative local pressure fluctuation called 'Variable Friction Coefficient' (VFC) for the flow transients is also incorporated into the model. For the accurate modeling of wave propagation, the split-coefficient matrix (SCM) method for characteristic-direction based splitting of eigenvalues is used in the study. The results show that the proposed two-equation model can reproduce the results from the three-equation model at a substantially reduced computational cost. The integration of the variable friction coefficient into the two-equation compressible-liquid model further improved the solver capability. The results computed using this aggregate solver are superior to the original three-equation model and the two-equation model without VFC. The results also suggest that the variable friction coefficient imparts adaptive damping capability to the solver model. This feature of the model is visible in the improved accuracy in the modeling of decaying pressure waves. The aggregate solver model, i.e., 'the variable friction coefficient integrated two-equation compressible-liquid model,' offers a greatly simplified mathematical model and an inexpensive computational solver for the simulation of hydraulic surges in non-cavitating flow transients.

doi: 10.5829/ije.2020.33.10a.23

1. INTRODUCTION

The hydraulic surge in pipes is a widely studied flow phenomenon in fluid dynamics due to its high practical relevance in the safety of water-supply for industrial and irrigation applications. Theory and experiments on fluid transients in systems and the studies on the various parameters affecting water hammer is available in [1]. The non-linear oscillations in visco-elastic pipelines conveying fluid is mathematically simulated in [2]. Modelling and optimizing hydraulic transients in water distribution systems, using the classical gradient and heuristic optimization techniques is reported in [3]. The study [4] analyses and designs surge tank, a device used to mitigate the effects of valve closure induced water hammer. Measurement systems like the optical-based

device presented in [5], shall soon lead to precisely recorded hydraulic surge data. Numerical modeling plays a significant role in the detection of destruction under the influence of cavitation. The pressure fluctuations on the bed of the compound flip buckets of a dam spillway are experimentally and numerically investigated in [6] and [7]. Numerical detection of cavitation damage level and location on dam spillways is presented in [8]. Corrosion is another factor that determines the safety of pipelines, and the protection systems are essential against corrosion, especially for oil and gas pipelines [9].

In most of the two-phase cavitation models like those studied in [10] and [11], the gaseous components are modeled as compressible fluids, whereas, the liquid component, which is usually water, is invariably treated to be incompressible. There are many practical situations where considering the liquid compressibility, though

*Corresponding Author Email: jishnuchandran@gmail.com
(R. J. Chandran)

mild, may contribute to the completeness of the model. Simulation of transient flows in visco-elastic pipes with vapor cavitation reported in [12] employs a compressible model for both the liquid and gaseous phases. For hydraulic surges arising from sudden valve closures at high operating pressures, the cavitation effects are generally absent. For such cases, a comparatively simple mathematical model is preferred, which drastically reduces the computational cost to simulate the flow transient.

In this work, a simplified mathematical model is presented, which is computationally inexpensive to model non-cavitating hydraulic surges. The prescribed model addresses the compressibility effects in the liquid handled in addition to the savings offered in computation. Another innovation in this work is the incorporation of a variable friction coefficient to the model to improve the prediction of transient surge pressure variation. This new friction coefficient is introduced as a function of local pressure fluctuation with the aim to adapt to the local requirements of wave damping.

The following section outlines the research methodology employed. The subsequent section presents the two-equation model, which includes the details of the liquid's compressible treatment and the defining of the variable friction coefficient. The mathematical formulation and the corresponding computational strategy used to develop the solver are detailed in Section 4. Section 5 describes the problem setup and selection of the computational domain. The numerical results for the transient cases from the simulation are thoroughly analyzed and are compared against their corresponding experimental values in the results and discussion section.

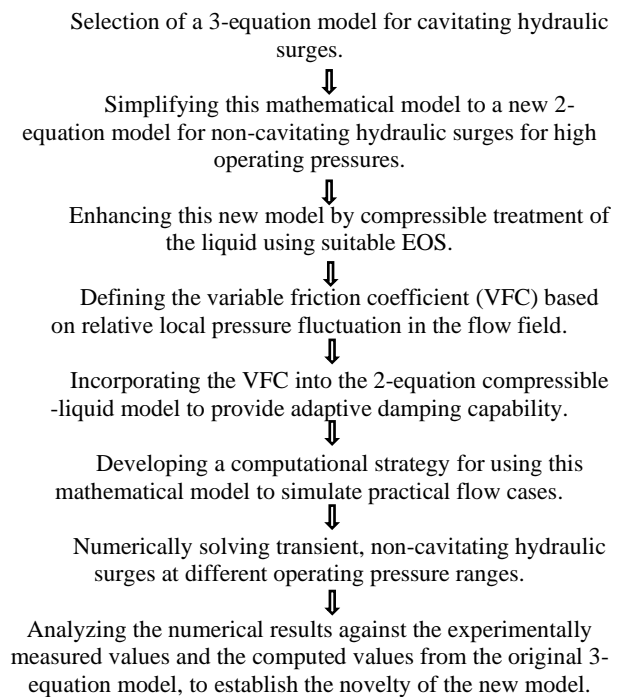
2. RESEARCH METHODOLOGY

A three-equation model is presented by Neuhaus et al. in [13] for calculations of thermo-hydraulic pressure surges in pipes. A modification to this model, a two-equation single-phase model, is presented in this study for hydraulic surge estimation for high-pressure flow cases where cavitation effects are negligible. The proposed single-phase model incorporates an equation of state (EOS) to take into account the compressibility effects of the liquid. The EOS relates the fluid density and signal wave speed to its pressure. The specific EOS we have used is the Modified Noble-Abel Stiffened Gas equation of state (Modified NASG EOS) [14], which is a highly accurate non-isothermal EOS for liquid water. The work also presents a variable friction coefficient, defined in the form of a tunable function of local pressure, to improve the accuracy of the numerical solver.

The computational model presented in the study is used to simulate the hydraulic surge and related flow transients associated with sudden valve closure

experiments conducted at the Pilot Plant Pipework (PPP) test rig of Fraunhofer, UMSICHT, Germany [15]. The Split-Coefficient Matrix (SCM) method [16], which uses characteristic direction based splitting, is used for modeling the wave propagation during the fluid transient. This powerful solution technique for wave propagation related fluid flow problems, is used for the numerical solution of two-phase flow equations in [17], and for the study of axially coupled vibration response of a fluid-conveying pipeline excited by water hammer in [18].

The proposed computational model is validated against the experimentally measured values reported in [15]. The two-equation model is compared to the original three-equation model to showcase the model simplification and improvements in saving the cost of computation. The flow chart below shows the research methodology used.



3. THE TWO-EQUATION COMPRESSIBLE-LIQUID MODEL

A three-equation two-phase model is proposed in [13] for numerical simulation of the cavitation hammer and related thermo-hydraulic pressure surges. The three equations used in this mathematical model are: the conservation equations for mass for the liquid phase, the gas phase (air-vapour mixture), and a combined momentum equation for both the phases.

The flow model also incorporates steady and unsteady friction models, as well as the effects of degassing. The results from this mathematical model are validated

against a series of experiments at the Pilot Plant Pipework (PPP), Fraunhofer UMSICHT. The report [15] shows the results from the three-equation mathematical model performing well with two-phase flow cases at low operating pressures. For high operating pressures reported in [15], this model performs satisfactorily only with the incorporation of FSI into the model.

Here we propose a two-equation single-phase model as a modification to the three-equation model described in [13], for flow situations where no cavitation effects are present. The proposed model tries to simulate the flow physics without using the FSI algorithm in the model, which considerably reduces the computational complexity. For single-phase flow in a horizontal pipe, in the absence of cavitation effects, the three-equation model [13] discussed above reduces to a two-equation system as follows.

$$\frac{1}{a^2} \frac{\partial p}{\partial t} + \frac{u}{a^2} \frac{\partial p}{\partial x} + \rho \frac{\partial u}{\partial x} = 0 \quad (1a)$$

$$\frac{\partial u}{\partial t} + u \frac{\partial u}{\partial x} + \frac{1}{\rho} \frac{\partial p}{\partial x} = -\frac{4\tau}{\rho d} \quad (1b)$$

where p , u , and ρ , and are respectively the pressure, axial velocity and density of the flow. The symbol a represents the speed of propagation of wave in the medium and τ is the shear force due to skin friction and d is the pipe diameter. The variables x and t denotes the spatial and temporal coordinates.

Equation (1a) represents the mass balance for the liquid, and the Equation (1b) represents the momentum balance for the liquid phase. The mass balance for gas phases identically satisfies due to the single-phase consideration. Equations (1a) and (1b) form a system of PDEs with the dependent variables u , p , and ρ . The temperature is assumed to be constant during the flow process, and the energy balances are thus automatically satisfied. The density ρ of the liquid is treated as a variable using an appropriate compressible model, as discussed in section 3.1, and the shear stress τ is estimated using an unsteady friction model, as explained in section 3.2.

3. 1. The Compressible Model for Water In the present study, water is modeled as a compressible liquid as it is subject to high pressures both at operating and surge conditions. The density of liquid water is estimated using the modified NASG equation of state (EOS) proposed in [14]. This EOS relates the pressure p , the specific volume v , and the specific internal energy ε of the liquid as follows:

$$p = (\gamma - 1) \frac{(\varepsilon - q)}{(v - b)} - \gamma p_\infty \quad (2)$$

In Equation (2) γ is the ratio of specific heats, p_∞ is the stiffening parameter, q is the heat bond of liquid water and b represents the covolume of the fluid. The relation

for speed of sound in unconfined liquid compatible with the EOS is given by Equation (3) as follows

$$c = \sqrt{\frac{\gamma v^2 (p + p_\infty)}{v - b}} \quad (3)$$

Radial expansion of the pipe is considered while estimating the speed of propagation of wave (a) in water, using the following relation

$$a = \frac{1}{\sqrt{\frac{1}{c^2} + (1 - \nu^2) \frac{\rho d}{Es}}} \quad (4)$$

In Equation (4), ν and E are respectively the Poisson's ratio and the Youngs modulus of pipe material, and s is the pipe wall thickness.

3. 2. The Variable Friction Coefficient It is a common observation that in the modeling of fluid hammer problems, discrepancies arise in the numerically computed data over the experimental or field data measured while using a steady shear stress model [19, 20]. Daily et al. [21] conducted laboratory experiments and found that these discrepancies are positive for accelerating flows and are negative for decelerating flows. A detailed review of the wall shear stress models used in the modeling of hydraulic transients is available in [22]. The relation of energy loss coefficient with transition geometry of a pipe, flow Reynolds number, and the relative roughness of the wall are outlined in [23]. The unsteady shear stress model used with the three-equation model in [13] takes the following form for single-phase liquid flow case as given by Equation (5).

$$\tau = \left(k \frac{\rho d}{4} a \right) \text{sign}(u) \frac{\partial u}{\partial x} \quad (5)$$

where k is the unsteady friction coefficient accounting for damping of pressure waves.

Daily et al. further showed that, for an unsteady shear stress model of the form of Equation (5), the coefficient k is a measure of the deviations due to unsteadiness of the wall shear and momentum flux. The extended thermodynamics approach by Axworthy et al. [24] supports this claim and reports the poor agreement between model and data while using a constant k value.

This study is further extended by replacing the pressure wave damping coefficient, k , by a variable friction coefficient, k_v . Unlike the constant coefficient, k , the new coefficient, k_v , is a function, which uses the ratio of the magnitude of local pressure fluctuations to the maximum possible pressure fluctuation for the cases considered. For the initial operating conditions of pressure p_0 , density ρ_0 , velocity u_0 , and signal speed a_0 , the magnitude of maximum possible pressure fluctuation Δp_{max} is computed using the well established Joukowsky equation as follows:

$$\Delta p_{max} = \rho_0 a_0 \Delta u = \rho_0 a_0 |u_0 - 0| = \rho_0 a_0 |u_0| \quad (6)$$

The importance of Joukowsky relation given by Equation (6) in the theory of water hammer is outlined in [25]. A similar non-dimensional parameter is defined in [26], using the Joukowsky pressure rise, to study the wave attenuation in fluid transients.

The magnitude of fluctuation in pressure at any local point 'i' is calculated as the absolute value of the difference between the local pressure p_i and the operating pressure p_0 . The variable friction coefficient, k_v is thus defined as:

$$k_v = m_1 \left[1 - \left(\frac{|p_i - p_0|}{\Delta p_{max}} \right)^{m_2} \right] \tag{7}$$

In Equation (7), m_1 and m_2 are tunable parameters. With this definition of the variable friction coefficient, k_v , the equation for shear stress can be written as:

$$\tau = \left(k_v \frac{\rho d}{4} a \right) \text{sign}(u) \frac{\partial u}{\partial x} \tag{8}$$

The shear stress computed from Equation (8) is used to estimate the source term in Equation (1b). The newly introduced variable friction coefficient, which uses the ratio of the local pressure fluctuations, which is transiently varying quantity, is expected to take care of the deviations due to unsteadiness, of the wall shear, and momentum flux to some extent.

4. MATHEMATICAL MODEL AND COMPUTATIONAL STRATEGY

The two-equation model is initially converted to the corresponding matrix form, and the resulting matrix system is then solved in a two-step process. The process involves converting the governing equations into characteristic form and solving them using the split coefficient matrix technique. The details are as given below.

4.1. Mathematical Model in Matrix Form

The governing relations of the two-equation model given by Equations (1a) and (1b) can be written in the compact matrix form as:

$$\begin{bmatrix} \frac{1}{a^2} & 0 \\ 0 & 1 \end{bmatrix} \begin{bmatrix} \frac{\partial p}{\partial t} \\ \frac{\partial u}{\partial t} \end{bmatrix} + \begin{bmatrix} \frac{u}{a^2} & \rho \\ \frac{1}{\rho} & u \end{bmatrix} \begin{bmatrix} \frac{\partial p}{\partial x} \\ \frac{\partial u}{\partial x} \end{bmatrix} = \begin{bmatrix} 0 \\ \frac{-4\tau}{\rho d} \end{bmatrix} \tag{9}$$

Equation (9) is of the form:

$$A \frac{\partial U}{\partial t} + B \frac{\partial U}{\partial x} = S \tag{10}$$

In Equation (10), the matrices and vectors are as in Equation (11)

$$A = \begin{bmatrix} \frac{1}{a^2} & 0 \\ 0 & 1 \end{bmatrix}, B = \begin{bmatrix} \frac{u}{a^2} & \rho \\ \frac{1}{\rho} & u \end{bmatrix}, S = \begin{bmatrix} 0 \\ \frac{-4\tau}{\rho d} \end{bmatrix}, U = \begin{bmatrix} p \\ u \end{bmatrix} \tag{11}$$

Premultiplying Equation (10) by A^{-1} , we obtain the following standard form in Equation (12)

$$\frac{\partial U}{\partial t} + C \frac{\partial U}{\partial x} = A^{-1}S \tag{12}$$

From the coefficient matrices A and B , the corresponding Jacobian matrix C and the eigenvalue matrix Λ are obtained as follows:

$$C = A^{-1}B = \begin{bmatrix} u & \rho a^2 \\ \frac{1}{\rho} & u \end{bmatrix} \text{ and } \Lambda = \begin{bmatrix} u - a & 0 \\ 0 & u + a \end{bmatrix} \tag{13}$$

Splitting the Jacobian matrix C in Equation (13) into left and right eigenvectors (Z and Z^{-1}), we obtain

$$C = Z \Lambda Z^{-1} = \begin{bmatrix} -\rho a & \rho a \\ 1 & 1 \end{bmatrix} \begin{bmatrix} u - a & 0 \\ 0 & u + a \end{bmatrix} \begin{bmatrix} -\frac{1}{2\rho a} & \frac{1}{2} \\ \frac{1}{2\rho a} & \frac{1}{2} \end{bmatrix} \tag{14}$$

In the first step of computation, the source term is excluded from Equation (12) and the resulting equation takes the form

$$\frac{\partial U}{\partial t} + C \frac{\partial U}{\partial x} = 0 \tag{15}$$

The split form of the Jacobian matrix C from Equation (14) is substituted into Equation (15). The resulting equation is premultiplied by Z^{-1} to obtain the following equation

$$Z^{-1} \frac{\partial U}{\partial t} + \Lambda Z^{-1} \frac{\partial U}{\partial x} = 0 \tag{16}$$

Defining the characteristic vector W as given in [27], such that

$$\partial W = Z^{-1} \partial U \tag{17}$$

Equation (16) changes to the following relation

$$\frac{\partial W}{\partial t} + \Lambda \frac{\partial W}{\partial x} = 0 \tag{18}$$

Linearizing Equation (17) similar to [28] we can compute the characteristic variable vector W using Equation (19)

$$W = Z^{-1}U = \begin{bmatrix} -\frac{p}{2\rho a} + \frac{u}{2} \\ \frac{p}{2\rho a} + \frac{u}{2} \end{bmatrix} \tag{19}$$

Equation (15) is thus transformed to the corresponding characteristic form in Equation (18).

4. 2. The Two-step Computational Algorithm

The solution of the two-equation model given by Equation (10) is obtained in a two-step process. In the first step, the system of equations in the characteristic form excluding the source terms given by Equation (18), is solved for an intermediate time step denoted by t^* starting from the n^{th} time step. The semi-discretized form of this equation for the i^{th} spatial grid is as follows:

$$W_i^* = W_i^n - \Delta t \left[\Lambda \frac{\partial W}{\partial x} \right]_i^n \quad (20)$$

The split coefficient matrix (SCM) method is used for solving the above system in Equation (20). The SCM method is used to split the eigenvalue matrix Λ into characteristic speed matrices with the positive and negative eigenvalues separated into the respective matrices Λ^+ and Λ^- as follows

$$\Lambda^+ = \frac{\Lambda + |\Lambda|}{2} \quad \text{and} \quad \Lambda^- = \frac{\Lambda - |\Lambda|}{2} \quad (21)$$

Using Λ^+ and Λ^- from Equation (21), the properties are updated to the intermediate time step as follows

$$W_i^* = W_i^n - \frac{\Delta t}{\Delta x} \left[\Lambda^+ \left(\frac{\partial W}{\partial x} \right)^- + \Lambda^- \left(\frac{\partial W}{\partial x} \right)^+ \right]_i^n \quad (22)$$

An explicit third-order upwind method is used for spatial discretization of the convective terms in Equation (22).

On completion of the first step of computation, the primitive variable vector is recovered from the characteristic variable vector as $U_i^* = ZW_i^*$. In the second step, the effect of the source term is integrated into the solution by retaining only the transient and source terms in Equation (10) as follows

$$\frac{\partial U}{\partial t} = A^{-1}S \quad (23)$$

and the semi-discretized form of Equation (23) is given below in Equation (24)

$$U_i^{n+1} = U_i^* + \Delta t [A^{-1}(U_i^n)S(U_i^n)] \quad (24)$$

Since there is no source term in the mass balance equation for liquid, only the momentum equation needs to be solved in the source term integration step. From the momentum equation, the velocity of flow is updated as

$$u_i^{n+1} = u_i^* - \Delta t \left(\frac{4\tau}{\rho d} \right) \quad (25)$$

In Equation (25), u^* is the component of the primitive variable vector U^* .

5. PROBLEM SET-UP AND COMPUTATIONAL DOMAIN

The experimental data used for validation of the mathematical model are from two high-pressure experiments conducted by Neuhaus et. al [15] at the Pilot Plant Pipework (PPP) test rig at Fraunhofer UMSICHT.

The schematic of the PPP experimental setup with measurement points is shown in Figure 1.

Demineralized tap water from the reservoir B1 is pumped into a 110 mm inner diameter and 170 m long steel pipeline. This pumping initially pressurizes the entire pipeline to the high pressure maintained inside the reservoir. The valve located between the pressure transducers P02 and P03 closes almost instantaneously at $t = 0$ while the pump remains running. Due to the sudden closure of the valve, a strong rarefaction wave is generated towards the downstream of it. This wave traverses further downstream towards the reservoir B1. Vapor bubbles can form at locations where the fluid pressure goes below its vapor pressure. The rarefaction waves generated oscillate in the pipe system and undergo multiple reflections at the boundaries until they get completely dissipated.

The two high pressure experiments chosen for validation of the method are the Experiment No. 415 and Experiment No. 347 mentioned in [15]. The details of the experiments are provided in Table 1.

The valve closure Experiments No. 415 and No. 347 correspond to the operating pressure ranges of 19.65 bar and 12.50 bar, respectively, with the temperature close to 20°C. For these two high-pressure experiments, the lowest values of transient pressure measured are well above the saturation pressure of the liquid, due to which the effects due to cavitation are absent. The pressure transducer P03 shown in Figure 1, located at a distance of 0.2 m downstream of the valve, records the transient pressure data. Numerically computed results using the proposed model are validated against these experimentally measured data. The single-phase two-equation model can be used to simulate the

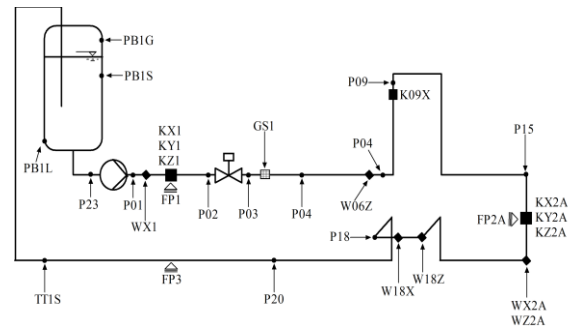


Figure 1. Schematic of the Fraunhofer UMSICHT PPP experimental setup with measurement points

TABLE 1. Details of the experimental conditions

Exp. No	Fluid Velocity, V [m/s]	Flow Rate, Q [m ³ /hr]	Temperature, T [°C]	Pressure, P_r [bar]
415	1.00	33.2	21.9	19.65
347	1.01	33.4	20.3	12.50

hydraulic surges in these two valve closure experiments, as both do not report cavitation effects.

The entire downstream side of the valve up to the reservoir B1, which is 149.4 m long, is the chosen computational domain. In our model, we have not considered the fluid-structure interactions in the pipe flow. A simplified one-dimensional straight pipe section of length 149.4 m is chosen for computation, as shown in Figure 2.

For the purpose of computation, the one-dimensional domain is divided into 747 uniformly sized control volumes, each of size $\Delta x = 0.2$ m. From the stability considerations, a CFL number of 0.03 is found to be optimal and the corresponding time step size Δt is calculated to be close to 5×10^{-6} s.

6. RESULTS AND DISCUSSION

A two-level performance analysis of the proposed two-equation model is presented in the study. In the first level, the two-equation model with compressible formulation for the liquid is evaluated against the experimentally measured data and the three-equation model of Neuhaus, which treats the liquid part as incompressible. In the second level of analysis, the variable friction coefficient is integrated into the two-equation compressible-liquid model, which is then compared for performance against the experimental results as well as the numerical results from the three-equation model. The detailed analyses of the results are provided below.

6. 1. The Two-equation Compressible-liquid Model with Constant Friction Coefficient

The transient flow problem of sudden valve closure in a steel pipe and the associated pressure surge are mathematically formulated using the proposed two-equation compressible-liquid model. This one-dimensional system of equations is solved numerically, and the results are compared against the numerical results computed using the existing three-equation model and with the transient pressure data measured experimentally. The experiment data were those measured using the pressure transducer P03 for Experiment Nos 415 and 347 reported in [15]. In the case of Experiment No. 415, the transient data measured for the first 3 s from the closure of the valve is used, while for Experiment No. 347, the measured data for the first 5 s is considered. The unsteady friction formulation reported in [13] is used with both the computational models. An optimized value of 0.18

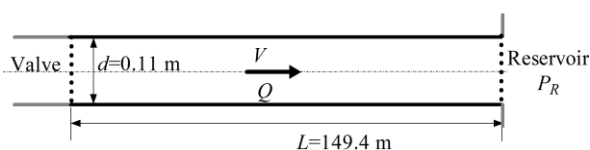


Figure 2. Schematic of the flow domain geometry and boundary conditions for computation

is used for the constant friction coefficient k in the simulation of these experiments.

In Figure 3, the continuous black color curve shows the experimentally measured transient pressure profile for Experiment No. 415. A strong rarefaction wave is generated just downstream of the valve immediately after its closure as the inertia of moving fluid creates a low-pressure area in the downstream region of the valve. The crests (peaks) and troughs (anti-peaks) seen from the experimental pressure profile indicate the rarefaction waves propagating back and forth along the length of the pipe, undergoing multiple reflections at the boundaries.

Due to frictional forces in the pipe flow system, these waves lose their energy and dissipate into a steady-state, which is evident from the decreasing amplitude of the pressure with time. The continuous blue colored curve in Figure 3 represents the transient pressure profile computed using the three-equation model [15]. Numerical results obtained from the present two-equation compressible-liquid model are displayed using the magenta colored curve in Figure 3.

For Experiment.No.347, the measured values of the transient pressure variation at the location P03 are shown using the continuous black curve in Figure 4.

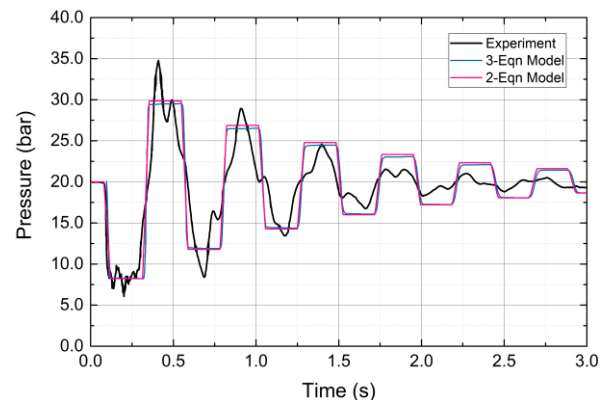


Figure 3. Comparison of measured and calculated pressure at P03 for experiment 415

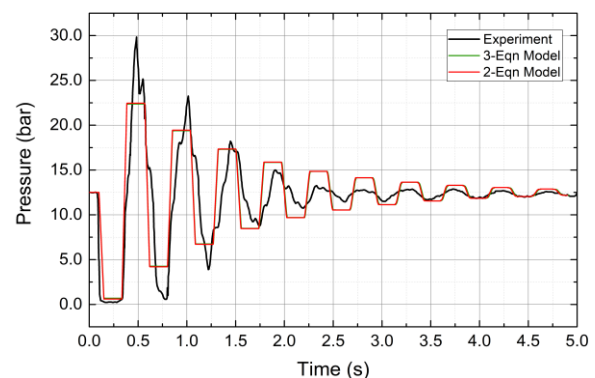


Figure 4. Comparison of measured and calculated pressure at P03 for experiment 347

The numerically computed transient pressure profiles using the three-equation and the two-equation models are shown in Figure 4 using the green colored and the red colored curves, respectively. As observed from Figures 3 and 4, the transient pressure profile predicted by the two-equation model proposed is in close agreement to that obtained from the existing three-equation model. However, one could notice that the two-equation model reproduced this numerical solution using a much simplified mathematical formulation, which requires considerably reduced computational effort.

On closer observation, one may find that the two-equation model predicts the peak pressures marginally higher than that of the three-equation model throughout the transient. This is visible in a better manner with Experiment No.415, as seen from Figure 3, which involves a comparatively high operating pressure. This increase in the pressure magnitude could be attributed to the compressible treatment of the liquid, which accounts for the increase in the density of the liquid at high pressures. The compressible treatment also leads to the accurate estimation of wave speeds within the fluid, which adds to the magnitude of the calculated surge pressure.

The computed frequency of the wave propagation is observed to be in close agreement with the experimental results. However, the amplitude of pressure peaks from the numerical results is not in good agreement with the measured values. The structural interactions with the fluid flow, which are not accounted for in the present model, is a possible reason for this disparity in the results. From the experimental and numerical pressure profiles displayed in Figures 3 and 4, an important observation is made as follows. During the initial phase of the transient, the magnitude of the pressure peaks and anti-peaks are highly under-predicted, and at the later phase, they are over-predicted in the numerical results. This observation is due to the over-damping induced by the constant friction coefficient for the initial transient phase and vice-versa. This improper damping technique using a constant friction coefficient, adds to the variation of the numerical results from the measured values.

6. 2. The Two-equation Compressible-liquid Model with Variable Friction Coefficient

A variable friction coefficient is proposed in this study to address the deficiencies of the constant friction coefficient model. The constant value of the friction coefficient, which is applied throughout the computation, makes it inflexible to the varying flow situations. This fixed amount of damping may prove to be excessive for a particular part of the transient while it may be insufficient for the rest. The definition of the varying friction coefficient k_v , which is a function of the relative local pressure fluctuation, has been outlined in section 3.2.

The magenta curve in Figure 5 and the red curve in Figure 6 displays the numerical results obtained with the

two-equation compressible-liquid model using the variable friction coefficient k_v for the Experiments 415 and 347, respectively.

In these figures, the numerical results from the two-equation model are compared against those computed using the three-equation model, and with the measured values from the corresponding experiments. The comparison reveals that the proposed two-equation model with the variable friction coefficient improves the result considerably from the three-equation model with a constant friction coefficient. This improvement is not only in terms of better estimation of peak pressures but also in closely reproducing the transient trend observed with experimental pressure measurements. The maximum pressure estimated by the new computational model using k_v is 1.18 bar (or 4%) higher for Experiment No.415 and by 1.22 bar (or 5.5%) higher for Experiment.No.347 when compared to the results from the three-equation model, which is reasonable improvement in quantitative terms. The proposed two-equation model can also reproduce the shape of the pressure profile much closer to the shape of the experimental profile by producing sharper peaks and anti-peaks. Values of the parameters m_1 and m_2 in Equation (9) are observed to be optimal in the range 0.3-0.5 for such experiments.

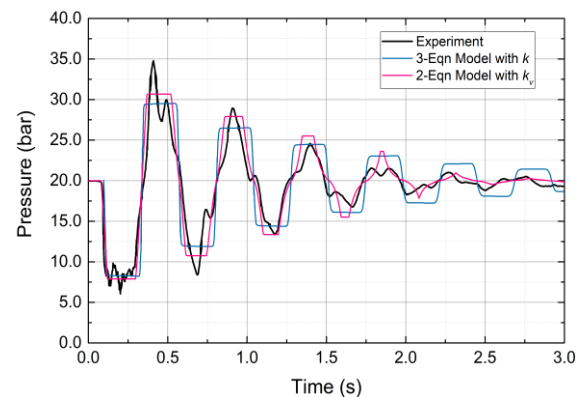


Figure 5. Numerical results from the 2-equation compressible model with k_v for Experiment No. 415

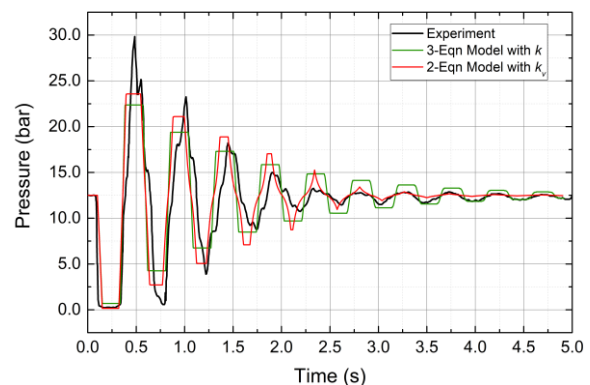


Figure 6. Numerical results using the 2-equation compressible model with k_v for Experiment No. 347

The damping provided by the variable friction coefficient is adaptive to the magnitude of pressure fluctuation at any local point. This capability is imparted through the unique function definition for k_v . It is visible from the numerical pressure profiles in Figures 5 and 6 that the variable friction coefficient provides low damping at the initial stage of the transient where larger pressure peaks are existent. Similarly, towards the later phase of the transient, the variable friction coefficient adapts to the pressure's diminishing magnitude. This adaptive damping capability improves the accuracy of the computed transient surge data, which is crucial to the pipe structure's safety. The flexibility added to the mathematical model by the variable friction coefficient to predict the numerical results close to measured data is notable, specifically towards the end of the transient in Figures 5 and 6.

The compressible model used for the liquid not only helps in the accurate prediction of the fluid density but also provides an excellent estimate of the wave speeds, both of which are crucial flow parameters varying with pressure. The proposed two-equation model, with the variable friction coefficient, is a highly simplified mathematical model capable of estimating the transient pressure variation accurately. This model's ability to follow the transient variations in the experimentally measured pressure profile, even without the inclusion of any fluid-structure interaction (FSI) algorithm, is a substantial improvement over the three-equation model.

There are visible variations in the numerical results during the initial stage of the transients. The main reason for these is that the effects of pipe mountings and support structures are neglected in the computational model. The lack of complete information regarding the exact nature of valve closure is another cause for any mismatches between the simulation results and the measured values. As observed from the experimental results, the maximum surge in pressure due to the sudden closure of the valve reaches much higher magnitudes than the operating pressure. The compressible model presented in the study, to a particular extent, could take this into account by relating these pressures to the corresponding liquid density and signal propagation speed. The variable friction coefficient also adds novelty to the model through the adaptive feature. Based on the above discussions, the proposed model is an efficient computational tool for modeling and prediction of pressure surges in flow systems where cavitation effects are absent.

7. CONCLUSIONS

A two-equation compressible-liquid model is developed for the simulation of non-cavitating hydraulic surges. The proposed model is limited to single-phase non-cavitating flow simulations. This model uses a suitable equation of

state to consider the compressibility effects in the liquid at high-pressure ranges. The model has the capability to accurately compute the fluctuations in density and wave speed in the liquid. The work also presents a uniquely defined variable friction coefficient, which is a function of the local pressure fluctuation. This new variable friction coefficient is superior to the constant friction coefficient that it adaptively damps the numerically computed transient pressure fluctuations. This adaptive damping capability helps the model to predict the transient pressure in a similar trend as observed with the experimentally measured data. The analysis reveals that the proposed model is computationally inexpensive and provides better accuracy in comparison to the three-equation model. The flexibility offered by a variable friction coefficient to the mathematical model in selectively treating transient pressure gradients is a significant contribution of this study. The two-equation compressible-liquid model with the variable friction coefficient is thus quantitatively and qualitatively superior to the existing model for computational applications for high-pressure pipelines for non-cavitating hydraulic surges. A possible future extension of this work is the incorporation of advanced numerical techniques for this model to provide high stability for transient two-phase flow modeling. The three-equation model as well can then be used with compressible-liquid and variable friction capabilities to model even cavitating hydraulic surges. Extending the use of the variable friction coefficient defined in this study to a wide variety of transient flow applications is another possible area of research.

8. REFERENCES

1. Bergant, A., Tijsseling, A.S., Vítkovský, J.P., Covas, D.I.C., Simpson, A.R. and Lambert, M.F., "Parameters affecting water-hammer wave attenuation, shape and timing-part 1: Mathematical tools", *Journal of Hydraulic Research*, Vol. 46, No. 3, (2008), 373-381. doi: 10.3826/jhr.2008.2848
2. Khudayarov, B., Turaev, F. "Mathematical simulation of nonlinear oscillations of viscoelastic pipelines conveying fluid". *Applied Mathematical Modelling*, Vol. 66, (2019), 662-679. doi: <https://doi.org/10.1016/j.apm.2018.10.008>
3. Skulovich, O., Perelman, L., Ostfeld, A. "Modeling and optimizing hydraulic transients in water distribution systems". *Procedia Engineering*, Vol. 70, (2014), 1558-1565. doi: <https://doi.org/10.1016/j.proeng.2014.02.172>
4. Moghaddam, M. A. "Analysis and design of a simple surge tank." *International Journal of Engineering Transactions A*, Vol. 17, No. 4, (2004), 339. doi: http://www.ije.ir/article_71544.html
5. Zamani, J., M. A. Samimi, F. Sardarzadeh, and M. H. Ghezelayagh. "An Optical Measurement System to Measure Velocity and Provide Shock Wave Pressure Diagrams.", *International Journal of Engineering*, Vol. 33, No. 3, (2020), 505-512. doi: 10.5829/ije.2020.33.03c.15
6. Yamini, O. A., Kavianpour, M. R., Mousavi, S. H., Movahedi, A., and Bavandpour, M. "Experimental investigation of pressure

- fluctuation on the bed of compound flip buckets." *ISH Journal of Hydraulic Engineering*, Vol. 24, No. 1, (2018), 45-52. doi: <https://doi.org/10.1080/09715010.2017.1344572>
7. Yamini, O. A., Kavianpour, M. R., and Movahedi, A. "Pressure Distribution on the Bed of the Compound Flip Buckets." *The Journal of Computational Multiphase Flows*, Vol. 7, No. 3, (2015), 181-94. doi:10.1260/1757-482X.7.3.181.
 8. Fadaei-Kermani, E., Barani, G. A., and Ghaeini-Hessaroeyeh, M. "Numerical Detection of Cavitation Damage on Dam Spillway." *Civil Engineering Journal*, Vol. 2, No. 9, (2016), 484-490. doi: 10.28991/cej-2016-00000051
 9. Nikitin, E., Shumatbaev, G., Terenzhev, D., Sinyashin, K., and Rastergaev, E. "New Sintanyl Phosphonates for Protection of Oil and Gas Pipelines from Steel Corrosion." *Civil Engineering Journal* Vol. 5, No. 4 (2019), 789-795. doi: 10.28991/cej-2019-03091288
 10. Sadafi, M., Riasi, A., Nourbakhsh, S.A. "Cavitating flow during water hammer using a generalized interface vaporous cavitation model". *Journal of Fluids and Structures*, Vol. 34, (2012), 190-201. doi: <https://doi.org/10.1016/j.jfluidstructs.2012.05.014>
 11. Pinho, J., Lema, M., Rambaud, P., Steelant, J. "Multiphase investigation of water hammer phenomenon using the full cavitation model". *Journal of Propulsion and Power*, Vol. 30, No. 1, (2014), 105-113. doi: <https://doi.org/10.2514/1.B34833>
 12. Hadj-Taieb, L., Hadj-Taieb, E. "Numerical simulation of transient flows in viscoelastic pipes with vapour cavitation". *International Journal of Modelling and Simulation*, Vol. 29, No. 2, (2009), 206-213. doi: <https://doi.org/10.1080/02286203.2009.11442526>
 13. Neuhaus, T., Dudlik, A. "Experiments and comparing calculations on thermohydraulic pressure surges in pipes". *Kerntechnik*, Vol. 71, No. 3, (2006), 87-94. doi: 10.3139/124.100280
 14. Chandran, R. J., Salih, A. "A modified equation of state for water for a wide range of pressure and the concept of water shock tube". *Fluid Phase Equilibria*, Vol. 483, (2019), 182-188. doi: <https://doi.org/10.1016/j.fluid.201811.032>
 15. Neuhaus, T., Dudlik, A., Tijsseling, A.S. "Experiments and corresponding calculations on thermohydraulic pressure surges in pipes". CASA-report 545. (2005). url: <https://research.tue.nl/files/2312420/602216.pdf>
 16. Chakravarthy, S., Anderson, D., Salas, M. "The split coefficient matrix method for hyperbolic systems of gasdynamic equations". In: 18th Aerospace Sciences Meeting. (1980), 268. doi: <https://doi.org/10.2514/6.1980-268>
 17. Wang, Z., Su, G., Qiu, S., Tian, W. "Preliminary study on split coefficient matrix method for two-phase flow equation solving". *Atomic Energy Science and Technology*, Vol. 49, No. 6, (2015), 1045-1050. Retrieved from: http://inis.iaea.org/search/search.aspx?orig_q=RN:48072547
 18. Zhang, T., Tan, Z., Zhang, H., Fan, J., Yang, Z. "Axial coupled response characteristics of a fluid-conveying pipeline based on split-coefficient matrix finite difference method". *Zhendong yu Chongji/Journal of Vibration and Shock*, Vol. 37, (2018), 148-154. doi: 10.13465/j.cnki.jvs.2018.05.022.
 19. Pezzinga, G., Ghidaoui, M.S., Axworthy, D.H., Zhao, M., McInnis, D.A. "Extended thermodynamics derivation of energy dissipation in unsteady pipe flow". *Journal of Hydraulic Engineering*, Vol. 127, No. 10, (2001), 888-890. doi: [https://doi.org/10.1061/\(ASCE\)0733-9429\(2001\)127:10\(888\)](https://doi.org/10.1061/(ASCE)0733-9429(2001)127:10(888))
 20. Ghidaoui, M.S., Mansour, S. "Efficient treatment of the vary-brown unsteady shear in pipe transients". *Journal of Hydraulic Engineering*, Vol. 128, No. 1, (2002), 102-112. doi: [https://doi.org/10.1061/\(ASCE\)0733-9429\(2002\)128:1\(102\)](https://doi.org/10.1061/(ASCE)0733-9429(2002)128:1(102))
 21. Daily, J., Hankey Jr, W., Olive, R., Jordaen Jr, J. "Resistance coefficients for accelerated and decelerated flows through smooth tubes and orifices". *Tech. Rep.; Massachusetts Inst of Tech Cambridge*. (1955). url: <https://apps.dtic.mil/dtic/tr/fulltext/u2/a280851.pdf>
 22. Ghidaoui, M.S., Zhao, M., McInnis, D.A., Axworthy, D.H. "A Review of Water Hammer Theory and Practice". *Applied Mechanics Reviews*, Vol. 58, No. 1, (2005), 49-76. doi: <https://doi.org/10.1115/1.1828050>
 23. Nosrati, K., Tahershamsi, A., and Taheri, S. H. S. "Numerical Analysis of Energy Loss Coefficient in Pipe Contraction Using ANSYS CFX Software." *Civil Engineering Journal* Vol. 3, No. 4 (2017): 288-300. doi: 10.28991/cej-2017-00000091
 24. Axworthy, D.H., Ghidaoui, M.S., McInnis, D.A. "Extended thermodynamics derivation of energy dissipation in unsteady pipe flow." *Journal of Hydraulic Engineering*, Vol. 126, No. 4, (2000): 276-287. doi: [https://doi.org/10.1061/\(ASCE\)0733-9429\(2000\)126:4\(276\)](https://doi.org/10.1061/(ASCE)0733-9429(2000)126:4(276))
 25. Ghidaoui, M. S. "On the fundamental equations of water hammer". *Urban Water Journal*, Vol. 1, No. 2, (2004), 71-83. doi: <https://doi.org/10.1080/15730620412331290001>
 26. Wahba, E. "Modelling the attenuation of laminar fluid transients in piping systems". *Applied Mathematical Modelling*, Vol. 32, No. 12, (2008), 2863-2871. doi: <https://doi.org/10.1016/j.apm.2007.10.004>
 27. Toro, E. "Riemann Solvers and Numerical Methods for Fluid Dynamics: A Practical Introduction". *Springer Berlin Heidelberg*; (2013). ISBN 9783662039151. doi: 10.1007/b79761
 28. Peng, J., Zhai, C., Ni, G., Yong, H., Shen, Y. "An adaptive characteristic-wise reconstruction weno-z scheme for gas dynamic euler equations". *Computers & Fluids*, Vol. 179, (2019), 34-51. doi: <https://doi.org/10.1016/j.compfluid.2018.08.008.19>

Persian Abstract

چکیده

هدف این تحقیق ارائه یک مدل دومعادله‌ای و محاسباتی کارآ برای یک سیال تراکم‌پذیر است. این مدل به‌طور خاص برای محاسبه‌ی عددی موج‌های هیدرولیکی در لوله‌های سیال تحت فشار بالا که در آن کاویتاسیون وجود ندارد، ایجاد شده است. هدف از ارائه‌ی این مدل ساده‌تر کردن مدل سه‌معادله‌ای نیوهاوس (Neuhaus) و همکاران برای ضربه‌ی قوچ (چکش کاویتاسیون) سیال دوفازی است. اثرات تراکم‌پذیری در مایع در طول گذار با بهره‌گیری از معادله‌ی حالت مناسب در مدل در نظر گرفته می‌شود. یک تابع تنظیم‌پذیر از نوسانات فشار نسبی موضعی به نام "ضریب اصطکاک متغیر" (VFC) برای جریان‌های گذرا نیز در مدل گنجانیده شده است. برای مدل‌سازی دقیق انتشار موج از روش ماتریس ضریب تقسیم (SCM) برای تقسیم بر اساس مقادیر ویژه در این مطالعه استفاده شده است. نتایج نشان می‌دهد که مدل دومعادله‌ای پیشنهادی می‌تواند نتایج حاصل از مدل سه‌معادله‌ای را با کاهش چشم‌گیری در هزینه‌های محاسباتی به دست آورد. ادغام ضریب اصطکاک متغیر در مدل مایع تراکم‌پذیر دومعادله‌ای قابلیت حل را بیشتر بهبود می‌بخشد. نتایج محاسبه شده با استفاده از این حل‌کننده‌ی کل نسبت به مدل اصلی سه‌معادله‌ای و مدل دومعادله‌ای بدون VFC برتری دارد. نتایج همچنین حاکی از آن است که ضریب اصطکاک متغیر قابلیت میرایی سازگاری را با مدل حل‌کننده ارائه می‌دهد. این ویژگی مدل در بهبود دقت در مدل‌سازی امواج فشار میرا قابل مشاهده است. مدل حل کل به عنوان مثال: "ضریب اصطکاک متغیر یک‌پارچه مدل دو معادله‌ای مایع فشارپذیر یک مدل ریاضی بسیار ساده و یک حل‌کننده‌ی محاسباتی ارزان‌قیمت برای شبیه‌سازی موج‌های هیدرولیک در جریان‌های گذار بدون کاویتاسیون ارائه می‌دهد."
